Kinetics of Phase Separation in Binary Mixtures of Polystyrene and Poly(vinyl methyl ether) As Studied by Fluorescence Emission of Labeled Polystyrene

Fadhel Ben Cheikh Larbi,† Jean-Louis Halary,* and Lucien Monnerie

Laboratoire de Physicochimie Structurale et Macromolêculaire, Ecole Supérieure de Physique et Chimie Industrielles de la Ville de Paris, 10, rue Vauquelin, F-75231 Paris Cedex 05, France

Received March 22, 1990; Revised Manuscript Received July 20, 1990

ABSTRACT: The initial stages of phase separation in binary mixtures of polystyrene and poly(vinyl methyl ether) have been examined by using a fluorescence emission technique. The experiments were performed on a series of mixtures covering the entire composition range. Thus, both the spinodal decomposition mechanism in the unstable one-phase region and the nucleation and growth mechanism in the metastable regions were investigated. The rates of phase separation are shown to present a logarithmic dependence on time. Their initial values vary in accordance with the driving forces predicted by the relevant theories. Two polystyrene samples of different molecular weight ($\bar{M}_w$ = 35 000 and 233 000) were used in order to check the influences of blend viscosity and phase separation temperature on the kinetics of the processes. In the nucleation and growth regime, chain mobility is an important factor, and the observed behavior is quite well described by assuming the validity of the Williams–Landel–Ferry (WLF) equation.

Introduction

Much attention has been paid in recent years to the kinetics of phase separation in polymer blends, from both a theoretical and an experimental viewpoint. Theories were propounded to predict the decay of the one-phase state in the special case of a binary mixture of polymers; they are referred to as spinodal decomposition (SD) in an initially unstable system[1,2] and nucleation and growth (NG) in a metastable system.[3] Several studies were carried out in order to compare these predictions with experimental data. With the exception of an excimer fluorescence study,[4] scattering techniques were used to investigate the dynamics of the thermally induced phase separation in the blend polystyrene (PS)–poly(vinyl methyl ether) (PVME) selected as a model system.[5-7] An important point is that the phase decomposition behavior is simpler in the earliest stages of the process, well before the appearance of the coarsening process.[8] Consequently, it is advantageous to follow the kinetics when the system is subjected to small thermodynamic driving forces, i.e., to superficial quenches inside the two-phase region. In this regard, it is crucial (i) to know very precisely the phase boundaries (binodal and spinodal lines) and (ii) to follow the kinetics with a technique sensitive enough to detect phase separation on a molecular scale.

These two requirements appear to be met in the case of the system PS–PVME by using the technique of fluorescence emission of labeled polystyrene, discovered and developed in our laboratory.[9] Indeed, determination of the binodals using this approach was achieved with surprising accuracy over a very large range of polymer molecular weights,[10] and suitable estimates of the spinodals were given, especially for not too high molecular weights.[11] It was possible to derive the influences of polymer molecular weights and polydispersities on the location of the phase diagram (and mainly of its minimum) in the temperature–composition plane.[10] Furthermore, it was shown that the fluorescence emission technique provides us with information on a scale smaller than light scattering and comparable to small-angle neutron scattering.[12]

That is the reason why we applied the fluorimetric method to investigate the phase separation kinetics.[13] This paper reports on experiments performed on a series of PS–PVME blends ranging from 10 to 90% of PS with the aim of analyzing both the SD and NG processes. Two PS's with the same polydispersity but different molecular weights were used in the blend preparation in order to check the effect of the relevant changes in viscosity and boundary phase location.

Experimental Section

Blend Preparation. Commercial polymer samples were used in this study. PVME ($\bar{M}_n$ = 46 500, $\bar{M}_w$ = 99 000), PS(L) ($\bar{M}_n$ = 34 000, $\bar{M}_w$ = 35 700), and PS(M) ($\bar{M}_n$ = 220 000, $\bar{M}_w$ = 233 000) were purchased from Scientific Polymer Products, Polymer Labs Ltd., and Polysciences Inc., respectively.

Labeled polystyrenes, including one anthracene group in the middle of the chains, were the same as those used in previous studies,[9] i.e., PS*(l) ($\bar{M}_n$ = 27 300, $\bar{M}_w$ = 30 000) and PS*(m) ($\bar{M}_n$ = 230 000, $\bar{M}_w$ = 253 000).

Solutions of PVME/PS/PS* were prepared by dissolving under stirring appropriate amounts of dried PVME and PS in a solution of PS* in toluene. Next, films were cast on glass plates from the solutions and then dried in an oven under nitrogen at room temperature for 24 h followed by 24 h at 60 °C and finally under vacuum in order to remove all the solvent. PS* concentration in the solution was adjusted in order to label the films with ca. 6 ppm of anthracene groups.

The compositions of the films under study are given in Table I. Film codes account for the characteristics of PS (L or M) and of PS* (l or m) and for the PVME ratio. In order to check the influence of label concentration on the results, some additional films containing PS*(m) were labeled with 35 ppm of anthracene groups. They are distinguished from the others by the code m$^+$ instead of m.

Glass Transition Temperature T_g. Measurements were performed by differential scanning calorimetry on a Du Pont 1090 calorimeter. The heating rate was 5 °C min^{-1}. T_g was conventionally taken as the intercept of the base line with the tangent to the experimental trace at the inflection point.

Fluorescence Measurements. Measurements were carried out under continuous illumination by using a fluorescence microscope with excitation and fluorescence emission wavelengths around 365 and 440 nm, respectively. As detailed in the previous

* To whom correspondence should be addressed.
† Present address: Department of Physics, Faculty of Sciences, Sfax, Tunisia.

0024-9297/91/2224-0867$02.50/0

Table I
Composition of the PVME/PS/PS* Films

	PVME, wt %	other components	T_{coex}, °C		PVME, wt %	other components	T_{coex}, °C
Ll2	79.4	PS(L) and PS*(l)	157	Ml1	90.0	PS(M) and PS*(l)	113.5
Ll3	70.3		152.5	Ml2	79.5		112.5
Ll4	59.9		150	Ml3	69.2		113
Ll5	50.0		148.5	Ml4	58.3		114.5
Ll6	41.2		148.5	Ml5	48.0		116.5
Ll7	30.0		149.5	Ml6	44.5		117.5
Ll8	20.4		151.5	Ml7	28.6		126.5
				Ml8	20.0		133.5
Lm2	80.0	PS(L) and PS*(m)	157	Mm1	90.0	PS(M) and PS*(m)	113.5
Lm5	50.0		148.5	Mm2	80.0		112.5
Lm8	90.0		151.5	Mm7	30.0		126.5

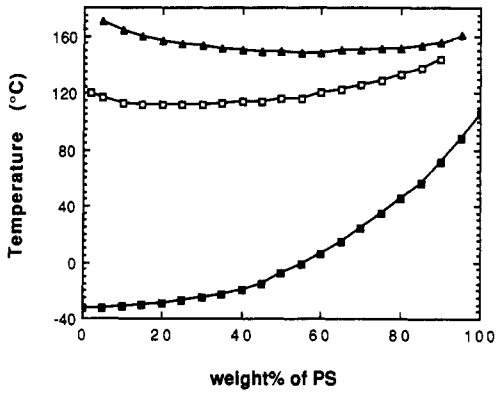

Figure 1. Plots of T_{coex} of system L (Δ), T_{coex} of system M (□), and T_g of both systems (■) versus polystyrene weight percentage in the blends.

papers of the series,[9] phase separation is detected in the form of a sharp upturn in fluorescence intensity.

Coexistence temperatures T_{coex} were determined with confidence by following a two-stage procedure. At first, they were estimated under continuous heating at a rate of 0.2 °C min^{-1}. Then precise values (a little bit lower) were reached from isothermal experiments. T_{coex} is the temperature at which the change in fluorescence intensity is as small as detectable over a 30-min period. The temperatures T_{coex} thus obtained (Table I) were proven to depend neither on the PS* chain length nor on the percentage of PS* in the blend, in agreement with our previous statements.[9] They define the familiar phase diagrams shown in Figure 1.

The following procedure was used to determine phase separation kinetics. Samples of thickness around 60 μm were placed in a hot stage attached to the microscope, then heated very rapidly up to the temperature $T = T_{coex} + \Delta T$, and finally held in isothermal conditions. ΔT values ranged from 0.5 to 5.5 °C. Fluorescence intensity, I_F was recorded continuously during the experiments. Since we were not interested in the absolute values of I_F (which should depend on film thickness, blend composition, and PS* content) but rather in the evolution of I_F as a function of phase separation time, the data have been replotted by normalizing I_F to an arbitrary value of 100 at zero time, whatever the sample under study may be.

Results and Discussion

A typical plot of fluorescence intensity I_F versus phase separation time t at different quench deepnesses ΔT is given in Figure 2a. As shown in Figure 2b, a rapid cooling down to T_{coex} - 2 °C allows the fluoresence intensity to decay and recover its initial value. This observation, verified whatever ΔT may be, corroborates well the suitability of the experiments and confirms the reversibility of the stages of phase separation under study. Plots on Figure 2 are relative to the blend Ml7, but we have observed that all the blends under consideration behave similarly. It is worth pointing out that, in our experiments, the shape of the fluorescence intensity profile is the same

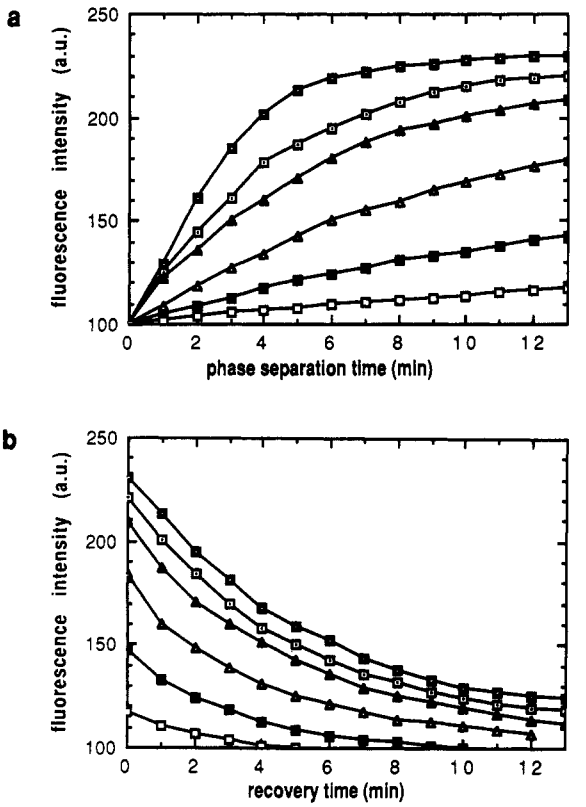

Figure 2. Blend Ml7 at different deepnesses of quench ΔT in the two-phase region (from top to bottom: ΔT = 5.5, 4.5, 3.5, 2.5, 1.5, and 0.5 °C): (a) phase separation profile; (b) recovery profile.

in the spinodal decomposition and in the nucleation and growth regimes.

The excess emission intensity, I_F - 100, exhibits a logarithmic increase with time and tends to a limiting value $I_{F\infty}$ at long enough phase separation time. In the same way, the decay profile of the quantity $I_{F\infty}$ is logarithmic. $I_{F\infty}$ can be determined with confidence by curve fitting at any deepness of quench ΔT. When this value of fluorescence intensity is attained, one can assume that the system has reached the late stage of phase decomposition. According to the description given by Hashimoto et al.,[14,15] the compositions of each phase are still the equilibrium compositions, and only the size of the domains is allowed to grow further with time. So being the case, the quantity $I_F - 100/I_{F\infty}$ yields the percentage of phase decomposition which has already occurred at time t. By applying to these data the methods commonly used for the analysis of chemical reaction kinetics, one derives first the demixing rates $v(t)$ from the slopes of the curves of I_F - 100 versus time and then the initial rate, v_0, from the value of the intercept with the y axis of the plot of $v(t)$ versus time (Figure 3). Since fluorescence intensities are normalized

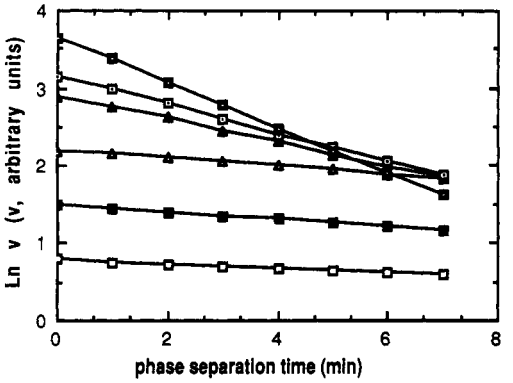

Figure 3. Plots of phase separation rates (calculated from data of Figure 2a) versus phase separation time.

with respect to $I_{F\infty}$, v_0 represents the percentage of phase separation per minute.

The values of v_0, determined at different ΔT, are given in Tables II and III for the series of blends L and M, respectively. Before we discuss these data, it is worth analyzing the possible influence on v_0 of the experimental conditions, namely, both chain length and concentration of PS*. Clearly, small differences are observed by comparing Tables II–IV, but the rates under consideration remain in the same range. As a matter of fact, these differences stay within the error bars on v_0 determinations.

From a qualitative viewpoint, two crude conclusions can be immediately derived from the inspection of the values of v_0 at any given $\Delta T = T - T_{coex}$: (i) rates of phase separation are faster when the PS chains in the blends are shorter, leading to a higher coexistence temperature; and (ii) for each series of blends, rate values differ markedly as a function of blend composition and pass systematically through a maximum in the regime of spinodal decomposition (SD) (blends Ml2 and Ll5, respectively). In some systems such as Ll6 or Ml3, the rate increase does not follow monotonously the increase in quench deepness, and the upturn reveals the transition from NG to SD phase separation mechanism.

The aim of quantitative analysis is to try to correlate for each blend the values of v_0, determined at different deepnesses of quench ΔT in the two-phase regions, with the corresponding driving forces predicted by the theoretical models.

Spinodal Decomposition. Let us consider first the spinodal decomposition regime in selecting the experimental data relative to blend compositions close to the thermodynamic critical composition. In our experiments with the series M and L, PS contents in the ranges 10–30% and 40–60%, respectively, provide reliable conditions for the spinodal decomposition mechanism to occur, and this, whatever ΔT may be. As blend composition moves away from the critical composition, the analysis has to be restricted to larger ΔT in order to neglect any contribution from the nucleation and growth mechanism. In contrast with early Pincus predictions,[2] it is now recognized from a theoretical viewpoint[16] that the initial growth rate of the fluctuations at the temperature T, $R(q)$, varies approximately as

$$R(q) \sim T\mu(\chi_s - \chi)q^2$$

In this relationship, q is the amplitude, supposed to be small, of the scattering vector and μ is a mobility factor accounting for chain dynamics effects. χ_s and χ are the values of the interaction parameter at the temperatures T and T_s, respectively; as shown in Figure 4, T_s is the temperature at which the spinodal curve is crossed. As a consequence, for a mean-field system, $R(q)$ should depend on temperature according to the simple relationship

$$R(q) \sim \mu(1/T_s - 1/T)$$

On condition that the mobility contribution can be neglected as a first approximation, $(T - T_s)/T_s$ is likely to be the thermodynamic driving force Δf_{SD} for spinodal decomposition. This conclusion is supported by different light scattering studies, including the pioneering paper of Snyder and Meakin.[5] Our fluorescence measurements are in agreement with these findings. As shown in Figure 5, a linear relationship is found by plotting the initial rate v_0 as a function of $(T - T_s)/T_s$. However, it is worth noting that this description holds only because attention is focused on initial rates (i.e., rates extrapolated to phase decomposition time $t = 0$) and also because the driving force (related to the deepness of quench ΔT in the two-phase domain) is moderate. Deviations from this simple behavior should be observed at higher ΔT and/or longer observation times.

Nucleation and Growth Regime. In the nucleation and growth regime, the situation is more complex in some respects. Very superficial quenches only are predicted to allow the system to obey classical nucleation theory.[17] As a consequence, experimental checks are difficult to perform owing to the lack of sensitivity of usual techniques in such conditions. Fortunately, this trouble does not exist when using the fluorescence quenching approach. In addition, the expression of the driving force, calculated by Binder,[3] is complicated. It can be conveniently separated in two terms, one of thermodynamic origin and the other dealing with chain dynamics aspects. The first term

$$\exp(\Delta f_{NG}) = \exp\left[N^{1/2}\left(\frac{T - T_c}{T_c}\right)^{1/2}\left(\frac{\phi_2 - \phi_1}{\phi_2 - \phi}\right)^2\right]$$

can be calculated from experimental data if phase diagram characteristics are known. Indeed, N is the average chain length, T is the phase separation temperature of the blend of initial volume fraction ϕ, T_c is the critical temperature (taken in approximation[11] as the minimum temperature of the coexistence curve), and ϕ_1 and ϕ_2 are the volume fractions (given by the coexistence curve) of the two phases in equilibrium at temperature T (see Figure 4). A peculiarity of the quantity Δf_{NG} is that it decreases with increasing ΔT. Figure 6 shows plots of log v_0 versus Δf_{NG} for different M and L blends, the composition of which is far away from the critical composition. As predicted by Binder's theory, straight lines are observed, but at very small ΔT only. For ΔT's larger than ca. 2 or 3 °C (depending on blend composition), deviations are observed in the form of a sharp increase in phase separation rates (left part of the plots). This may be the consequence of the transition from the nucleation and growth to the spinodal decomposition mechanism or, at least, of the appearance of the so-called spinodal nucleation[16] intermediate mechanism. It is worth noting at this point that requirements for theoretical predictions to be fulfilled are even more drastic in nucleation and growth than they are in spinodal decomposition conditions. The second term in Binder's theory may be written in the form (W/N^2) $\exp[-(\pi/4)f^3]$, where f is a constant of order of magnitude unity and the prefactor W is a quantity that cannot be worked out from experimental conditions but that is closely related to polymer chain dynamics. Inspection of v_0 values in each series M and L shows that the initial rate of nucleation and growth decreases when the volume fraction is increased. Two main factors may be involved to justify this observation from a qualitative point of view. First,

Table II
Initial Rates of Phase Separation v_0^a for Blends of the Series L at Different Quench Deepnesses ΔT

	deepness of quench ΔT, °C							
blend	0.5	1	1.5	2	2.5	3	3.5	4.5
Ll2		108		113		137		
Ll3	115		137		155		200	
Ll4		110		160		230		
Ll5	120		133		206		397	
Lm5	122		137		175		350	
Ll6	105		119		131		180	
Ll7	57		66		97		129	133
Ll8	28		29		41		52	110
Lm8	28		30		37		49	

[a] In units of percent demixing per minute.

Table III
Initial Rates of Phase Separation v_0^a for Blends of the Series M at Different Quench Deepnesses ΔT

	deepness of quench ΔT, °C								
blend	0.5	1.0	1.5	2.0	2.5	3	3.5	4.0	4.5
Ml1		29.8		34.5		45.6			74.0
Ml2		52.0		74.0		86.8			
Ml3		26.5		31.1		44.1		78.7	
Ml4	22.3		33.1		41				
Ml5	16.4		22.2		26.1		30.0		
Ml6	7.9				11.7		17.7	16.4	
Ml7	4.0		5.8		8.8		13.2	18.8	
Ml8	1.2		1.7		2.5		3.5		

[a] In units of percent demixing per minute.

Table IV
Initial Rates of Phase Separation v_0^a at Different Quench Deepnesses for Blends Labeled with PS*(m)

	deepness of quench ΔT, °C							
blend	0.5	1	1.5	2	2.5	3	3.5	4.5
Lm5	122		137		175		350	
Lm8	28		30		37		49	
Mm1		27		44		54		84
Mm*1		38.6		64		70		
Mm2		33		71.6		76.3		
Mm*2		46		51		65		
Mm*7	7		9		10.8		14	

[a] In units of percent demixing per minute.

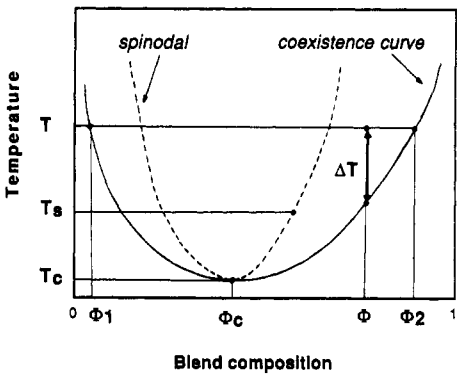

Figure 4. Schematic representation of the quantities involved in the expressions of the thermodynamic driving forces.

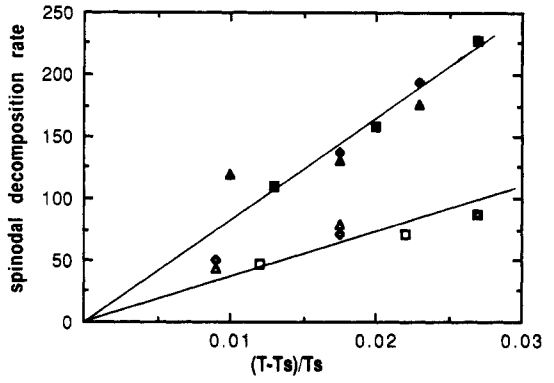

Figure 5. Spinodal decomposition initial rates of system L (open symbols) and system M (full symbols) versus $(T - T_s)/T_s$.

any increase in polystyrene concentration is accompanied by an increase in blend viscosity, since PS chains in the liquid state are more rigid than PVME chains. Second, as schematized in Figure 1, any increase in PS concentration allows phase separation to develop at temperatures closer and closer to the glass transition of the blend. As a consequence, chain mobility is slowed down and phase separation kinetics as well. Unfortunately, it is impossible to account for these two effects in a quantitative manner. In particular, it is difficult to evaluate the average chain length N with confidence, mainly because of (i) marked differences of molecular weight and polydispersity of the polymer samples under study in the present paper and (ii) ambiguity on PS and PVME equivalent segment length in the blends, as reported previously.[10] On the other hand, it is almost easy to discuss the influence of chain mobility on phase separation kinetics by direct comparison of two PS–PVME blends of the same PS volume fraction, but with one blend prepared with PS(L) and the other with PS(M). As an example, let us compare the blends Ll8 and Ml8, which are both in the nucleation and growth regime and which exhibit a difference between phase separation temperature and glass transition temperature of 105.5 and

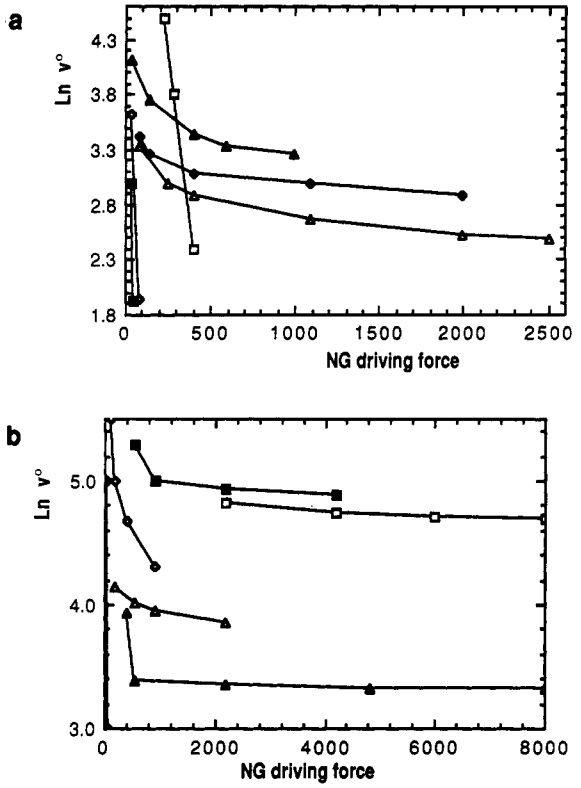

Figure 6. Nucleation and growth initial rates versus thermodynamic driving force Δf_{NG}: (a) system M; (b) system L.

86.5 °C, respectively (Figure 1). An estimate of the mobility effect can be provided by calculating what would be the rate of nucleation of growth if phase separation were appearing in blend Ll8 at a temperature of 86.5 °C only above the glass transition. The well-known WLF equation[18] is suitable for this calculation since it has been shown that PS, PVME, and their blends obey roughly the same time–temperature dependence.[19] As shown in Figure 7, the WLF correction leads to rate depressions of ca. 2 orders of magnitude, which correspond to values in reasonable agreement with the actual rates observed on the blend Ml8 at the same departure from T_g. Even if the roughness of this calculation is questionable, it shows unambiguously that the gap existing between phase separation temperature and glass transition temperature is a dominant factor regarding the rates of phase separation in the nucleation and growth regime.

Thus, the order of magnitude of phase separation rate depends mainly on dynamic chain aspects in the nucleation and growth regime, and changes in Δf_{NG} play a secondary role only. These conclusions, deduced from the analysis of the model system PS–PVME, are expected to be valid for any polymer blend exhibiting a LCST-type phase separation behavior.

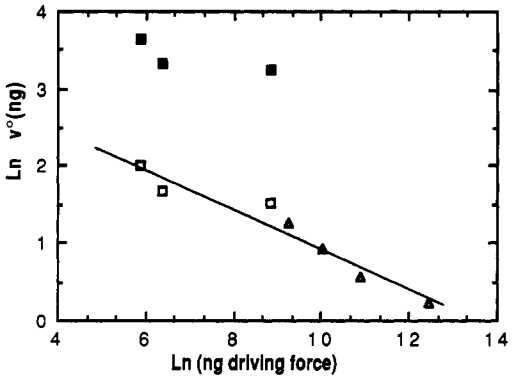

Figure 7. Nucleation and growth initial rates versus thermodynamic driving force Δf_{NG}: (Δ) blend Ml8; (■) blend Ll8; (□) blend Ll8 recalculated at $T - T_g = 86.5$ °C.

Acknowledgment. This study was supported by the Centre National de la Recherche Scientifique under Contract No. ATP 983018. We thank Prof. K. Binder (Mainz, Germany) for fruitful and stimulating discussions.

References and Notes

(1) de Gennes, P.-G. *J. Chem. Phys.* **1980**, *72*, 4756.
(2) Pincus, P. *J. Chem. Phys.* **1981**, *75*, 1996.
(3) Binder, K. *J. Chem. Phys.* **1983**, *79*, 6387.
(4) Gelles, R.; Frank, C. W. *Macromolecules* **1982**, *15*, 1486.
(5) Snyder, H. L.; Meakin, P. *Macromolecules* **1983**, *16*, 757.
(6) Han, C. C.; Okado, M.; Sato, T. in *Dynamics of Ordering Processes in Condensed Matter*; Komura, S., Furukawa, H., Eds.; Plenum Press: New York, 1988; p 433.
(7) Hashimoto, T. In *Dynamics of Ordering Processes in Condensed Matter*; Komura, S., Furukawa, H., Eds.; Plenum Press: New York, 1988; pp 421, 457.
(8) Lifchitz, I. M.; Slyozov, V. V. *J. Chem. Solids* **1961**, *19*, 35.
(9) Halary, J.-L.; Monnerie, L. In *Photophysical and Photochemical Tools in Polymer Science*; Winnik, M., Ed.; D. Reidel: Dordrecht, 1986; p 589.
(10) Ubrich, J. M.; Ben Cheikh Larbi, F.; Halary, J.-L.; Monnerie, L.; Bauer, B. J.; Han, C. C. *Macromolecules* **1986**, *19*, 810.
(11) Halary, J.-L.; Ubrich, J. M.; Nunzi, J. M.; Monnerie, L.; Stein, R. S. *Polymer* **1984**, *25*, 956.
(12) Halary, J.-L.; Ubrich, J. M.; Monnerie, L.; Yang, H.; Stein, R. S. *Polym. Commun.* **1985**, *26*, 73.
(13) Ben Cheikh Larbi, F.; Halary, J.-L.; Monnerie, L.; Williams, C. E. *Polym. Prepr. (Am. Chem. Soc., Div. Polym. Chem.)* **1987**, *28*, 122.
(14) Hashimoto, T.; Itakura, M.; Shimidzu, N. *J. Chem. Phys.* **1986**, *85*, 6773.
(15) Hashimoto, T.; Itakura, M.; Hasegawa, H. *J. Chem. Phys.* **1986**, *85*, 6118.
(16) Binder, K. In *Materials Science and Technology. Phase Transformations in Materials*; Haasen, P., Ed.; VCH: Weinheim, in press; Vol. 5, Chapter 5.
(17) Heermann, D. W.; Klein, W. *Phys. Rev.* **1983**, *B27*, 1732.
(18) Ferry, J. D. in *Viscoelastic Properties of Polymers*, 3rd ed.; Wiley: New York, 1980.
(19) Halary, J.-L.; Ben Cheikh Larbi, F.; Oudin, P.; Monnerie, L. *Makromol. Chem.* **1988**, *189*, 2117.

Registry No. PVME, 9003-09-2; PS, 9003-53-6.